Rotations of $4n\pi$ and the Kinematic Design of Parallel Manipulators

Joe Rooney*

Faculty of Mathematics, Computing and Technology, Open University, Milton Keynes, UK

Abstract: For parallel manipulator systems a fundamental distinction is drawn between displacement and motion. The former is a spatial relation adequately modelled by standard vector and matrix algebra. The latter is a spatial trajectory whose 'history' also requires modelling. Quaternion, spinor and Clifford algebra representations are utilised for this purpose - specifically for rigid body finite rotation in 3D space. Each involves rotation half-angles and hence exhibits apparently counter-intuitive features, notably that rotations of 0 and 2π are not equivalent, whereas rotations of 0 and 4π are equivalent. In general, rotations of $4n\pi$ are not equivalent to rotations of $(4n+2)\pi$, where n is any integer. These representations have real physical manifestations, demonstrated here for parallel manipulator designs, adapted from a mechanical model devised by Dirac.

Keywords: Parallel manipulator, $4n\ \pi$ spatial rotation, parametric ball, quaternion, spinor, multi-vector, clifford algebra, dirac.

1. INTRODUCTION

The kinematic design of parallel manipulator systems, whether cable-based [1], tensegrity-based [2], or rigid-link types [3], involves the representation of the shapes, the relative positions, and the motions of the links and joints. In particular, infinitesimal rotations of the platform and legs are commonly modelled by vector and matrix algebra. However, finite rotations have been represented mathematically in several different forms [4]. Of course the standard 3×3 matrix representations are commonly used here also, because of widely available software. But the unit quaternion representation has better computational efficiency and this has led to its extensive use in robotics, computer graphics, and space probe attitude control [4-7]. Similarly, related spinor and multi-vector representations are used in physics for conceptual reasons [8-10].

Unlike the standard 3×3 matrix representation, the quaternion, spinor and multi-vector representations each has the important feature of being expressed in terms of *half* the rotation angle, leading to the counter-intuitive conclusion that a rotation through an angle of 2π is not equivalent to a rotation through an angle of zero, but that a 4π rotation is equivalent to a zero rotation. They are considered to form a 'double cover' for the group of (finite) 3D rotations.

There is a physical reason for this double-cover representation that is recognised in quantum mechanics, and it turns out that there is a corresponding realisation in applied mechanics that may be demonstrated with a mechanical model. This was introduced by Dirac in the early 20th Century, to explain some features of electron spin [11]. It is adapted and presented here to draw attention to its potential use in the kinematic design of parallel manipulators. In general, manipulator platform rotations of $4n\pi$ are not equivalent to rotations of $(4n+2)\pi$, where n is any chosen integer (positive, negative or zero).

*Address correspondence to these authors at the Faculty of Mathematics, Computing and Technology, Open University, Milton Keynes, UK; Tel: +44 (0)1908 652979; Fax: +44 (0)1908 654052; E-mail: j.rooney@open.ac.uk

The conceptual difficulty lies with the meaning of 'rotation'. Is it just a *displacement*, in other words a spatial relation, relating, via a coordinate transformation, the initial pose A of a rigid body to the final pose B? Or, is it a *motion*, in other words an operation involving the 'history' of the actual path/trajectory taken from pose A to pose B? In either case it is a feature of the relationship between *two* bodies, and has no absolute meaning for a single isolated body. If 'rotation' means 'a type of spatial relation' then the geometrical juxtaposition of initial and final poses should be sufficient to represent it. However, if 'rotation' means 'a particular path or trajectory' then the topology of the process is also important in order to recognise if and when two or more distinct paths/trajectories are equivalent. In the former case a 2π rotation (or any multiple of 2π) is indistinguishable from a zero rotation, but in the latter case it turns out that these are essentially different and it requires a 4π rotation (or any multiple of 4π) for equivalence to a zero rotation.

2. REPRESENTING ROTATION: THE PARAMETRIC BALL

In 3D space a finite rotation has an axis and a magnitude. If the axis is considered to be a direction, then the combination of the rotation magnitude and the axis direction ostensibly defines a vector, visualised as a line segment located at some origin, lying along the direction of the axis and having a length equal to the (angular) magnitude [12, 13]. However, at least three aspects of this 'vector' viewpoint are vectorially atypical or misleading.

Firstly, a 3D finite rotation is associated with an axis *in some position*, and so the 'vector' representing it cannot be a *free* vector, unlike the case of a translation.

Secondly, this 'vector' representation does not preserve the structure of combinations of finite rotations about different axes. Combining two finite rotations about two non-parallel but intersecting axes, gives a resultant finite rotation that is not represented by the standard vector resultant of the two line segments representing the individual

1874-155X/10

finite rotations. For instance the axis of the resultant does not generally lie in the same plane as the axes of the two individual rotations. And furthermore if the original two axes are skew the resultant is not a rotation but a screw.

Thirdly, when considered as a spatial relation, the magnitude of a finite rotation is limited to a 2π range, such as $(0, 2\pi)$ or $(-\pi, \pi)$, on the real line. Hence the 'vectors' for all possible finite rotations about a fixed point are contained within the interior or boundary of a sphere of radius π. Moreover, each pair of diametrically opposite points on the surface of this sphere (and hence also the two radius 'vectors' to those points) must be identified, since, for example, a rotation of π about any axis direction represents the same spatial relation as a rotation of $-\pi$ about the same axis direction. Altmann [13] refers to this sphere as '*the parametric ball*'.

These problematical aspects have led to much confusion in understanding 3D finite rotations. However, the situation may be clarified by focusing on the *points* of the parametric ball and not on the *position 'vectors'* of its points. A given point within or on the surface of the parametric ball represents a rigid body in some fixed pose *A*. Any other point represents the same rigid body in a different fixed pose *B* (unless the second point is diametrically opposite the first point). The origin point may be taken to represent the rigid body in some reference fixed pose. The spatial relation between any two poses *A* and *B* is defined by the two sets of parameters for the positions of the two points representing the two poses, and not by, for instance, the difference of their position 'vectors'. One way to define the spatial relation between pose *A* and the origin pose is to specify its direction from the origin and the 'shortest' angular distance along this direction from the origin. This appears to be a position vector, but it behaves differently because of the atypical features discussed above.

A rigid body may reach a pose *A* from the origin, or change its pose from *A* to *B*, along an infinite number of different paths within the parametric ball. These paths should not be considered as displacement vectors even when they appear to be straight line segments, but rather should be considered to be directed curvilinear lines. The usefulness of the parametric ball representation stems from how it illuminates the inter-relationships amongst all these different possible paths. It turns out that there are just two essentially different *classes* of path from the point representing pose *A* to the point representing pose *B*, and the difference between the two classes is *topological* rather than geometrical. The paths are *homotopically* distinct. Within one homotopy class, any path, with end points *A* and *B*, may be continuously deformed into another path with the same end points without breaking the path into two or more disjoint parts. But a path from one homotopy class cannot be continuously deformed in this way into a path from another homotopy class.

Fig. (**1**) shows a plane cross-section of the parametric ball and illustrates the situation for three typical directed paths from some pose *A* to another pose *B*. The direction of each path is indicated by arrowheads, but the arrows do not signify vector quantities. The first path remains within the interior of the parametric ball, the second involves visiting the boundary of the parametric ball once, and the third involves visiting the boundary twice. Diametrically opposite points (such as *C* and *C*', or *D* and *D*') on the boundary are identified, and here, for clarity, *C* and *D* (and *C*' and *D*') are

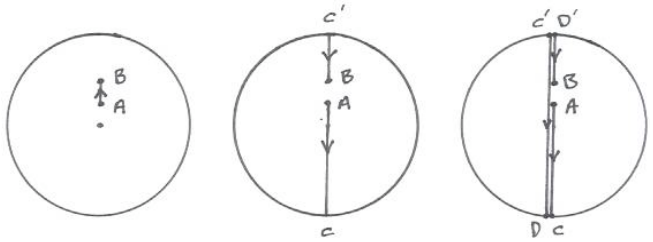

Fig. (1). Three paths in the parametric ball (radius π) from pose *A* to pose *B*.

shown as separate points. Each of the three paths involves a rotation about a fixed (vertical) axis, but this is not an essential feature. The first path may be deformed continuously into the third path but not into the second path. The first and third paths belong to the same homotopy class, whereas the second path belongs to a different homotopy class.

Fig. (**2**) shows the essential features of a typical *failed* attempt to deform the second path of Fig. (**1**) continuously into the first path, by varying the path in a continuous sequence of intermediate steps, each of which may involve a change in some rotation axis directions. These attempts always fail because the identified boundary points *C* and *C*' must always remain diametrically opposite.

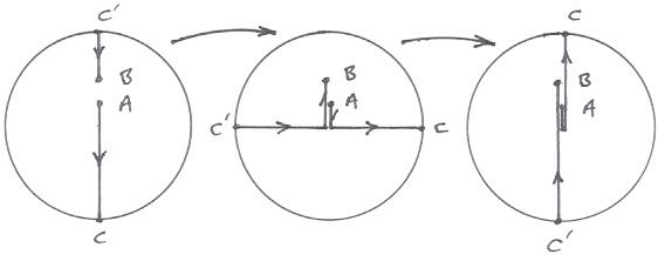

Fig. (2). Failed attempt to deform the second path of Fig. (**1**) into the first path.

Fig. (**3**) shows the essential features of a possible *successful* sequence to deform the third path of Fig. (**1**) continuously into the first path. For clarity at each step the segmented intermediate paths are chosen to be rotations about fixed axes (i.e. temporarily fixed radial lines from the origin of the parametric ball), but again this is not an essential feature. This time the attempt succeeds because there are two visits to the boundary and eventually at the end of the sequence various intermediate path segments are retraced in both directions, thereby cancelling each other completely, or at least partly.

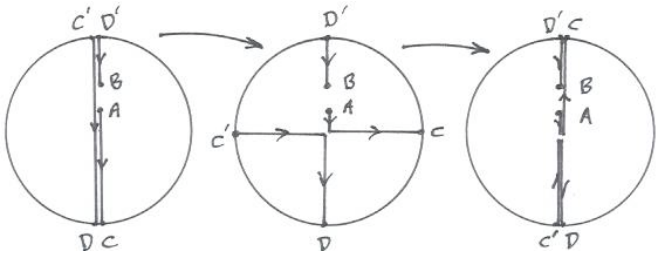

Fig. (3). Successful sequence to deform the third path of Fig. (**1**) into the first path.

Now suppose the two poses A and B to be identical and both to be located at the origin so that they represent a zero rotation about some (any) axis. The three directed paths in Fig. (**1**) would then represent paths from the origin back to itself. Again the first path (this time just the origin point) remains within the interior of the parametric ball, the second involves visiting the boundary of the parametric ball once, and the third involves visiting the boundary twice. As before the first and third paths will belong to the same homotopy class, whereas the second path belongs to a different class. If A and B were both at the origin a similar figure to Fig. (**2**) would still show a failed attempt to deform the second path continuously into the first. This demonstrates that a 2π rotation *is not* homotopically equivalent to a zero rotation. And of course a similar figure to Fig. (**3**) would still show a successful sequence to deform the third path continuously into the first. This demonstrates that a 4π rotation *is* homotopically equivalent to a zero rotation, but not to a 2π rotation. A mechanical realisation of these counter-intuitive features of 3D rotation is presented in section 5 and it has a direct bearing on cable-based parallel manipulators.

3. MATRIX, QUATERNION, SPINOR AND MULTI-VECTOR REPRESENTATIONS OF ROTATION

The commonest representation of a general 3D finite rotation, considered as a finite spatial displacement, is the following real orthogonal 3×3 matrix:

$$\mathbf{T}_{(l,m,n)}(\theta)=\begin{bmatrix} l^2(1-\cos\theta)+\cos\theta & lm(1-\cos\theta)-n\sin\theta & ln(1-\cos\theta)+m\sin\theta \\ ml(1-\cos\theta)+n\sin\theta & m^2(1-\cos\theta)+\cos\theta & mn(1-\cos\theta)-l\sin\theta \\ nl(1-\cos\theta)-m\sin\theta & nm(1-\cos\theta)+l\sin\theta & n^2(1-\cos\theta)+\cos\theta \end{bmatrix} \tag{1}$$

The familiar *matrix multiplication* operation:

$$\mathbf{r}' = \mathbf{T}_{(l,m,n)}(\theta)\mathbf{r} \tag{2}$$

effects the 3D finite rotation of a vector $\mathbf{r}\ (=x\mathbf{i}+y\mathbf{j}+z\mathbf{k})$ about an axis with direction cosines (l,m,n) through an angle θ into a new position $\mathbf{r}'\ (=x'\mathbf{i}+y'\mathbf{j}+z'\mathbf{k})$. Essentially this matrix representation encapsulates the geometry (but not the topology) of the spatial relation between the initial pose A of a rigid body and its final pose B after rotation. It involves the full rotation angle and is single-valued because:

$$\mathbf{T}_{(l,m,n)}(\theta+2\pi)=\mathbf{T}_{(l,m,n)}(\theta) \tag{3}$$

The symbol **T** (rather than **R**) is used here both to signify that it involves a coordinate transformation, and to distinguish it from the multi-vector representation dealt with below.

In the 19th Century, Hamilton [14] and Clifford [15] discovered different operations that could represent 3D finite rotations about an axis in space, but their representations did not just represent the finite spatial displacement - they also represented aspects of the motion trajectory. But a consequence of both new approaches was that they were double-valued in the rotation angle. Hamilton's approach involved a new type of (non-commutative) algebra based on a 4-tuple of real numbers (q_0,q_1,q_2,q_3) that he referred to as a *quaternion*. A general quaternion is usually written in the following form, involving the four quaternion *bases* $1,\mathbf{i},\mathbf{j},\mathbf{k}$:

$$\mathbf{q} = q_0 + q_1\mathbf{i} + q_2\mathbf{j} + q_3\mathbf{k} \tag{4}$$

where q_0 is a scalar and $q_1\mathbf{i}+q_2\mathbf{j}+q_3\mathbf{k}$ is a 3D vector. Hamilton constructed a *unit* quaternion (for which $q_0^2+q_1^2+q_2^2+q_3^2=1$) and utilised his non-commutative quaternion multiplication to effect the finite rotation of a 3D vector $\mathbf{r}\ (=x\mathbf{i}+y\mathbf{j}+z\mathbf{k})$ about an axis with direction cosines (l,m,n) through an angle θ into a new vector $\mathbf{r}'\ (=x'\mathbf{i}+y'\mathbf{j}+z'\mathbf{k})$, having the same magnitude as the first. The quaternion multiplication operation that produces a 3D finite rotation of a vector is given by:

$$\mathbf{r}' = \mathbf{q}(\theta)\mathbf{r}\mathbf{q}^{-1}(\theta) \tag{5}$$

Here the unit quaternion is:

$$\mathbf{q}(\theta) = \cos\frac{\theta}{2} + l\sin\frac{\theta}{2}\mathbf{i} + m\sin\frac{\theta}{2}\mathbf{j} + n\sin\frac{\theta}{2}\mathbf{k} \tag{6}$$

and its *inverse* is:

$$\mathbf{q}^{-1}(\theta) = \cos\frac{\theta}{2} - l\sin\frac{\theta}{2}\mathbf{i} - m\sin\frac{\theta}{2}\mathbf{j} - n\sin\frac{\theta}{2}\mathbf{k} \tag{7}$$

Table 1. Multiplication Rules for Products of Any Two of the Four Quaternion Bases

	i	**j**	**k**
i	-1	**k**	**-j**
j	**-k**	-1	**i**
k	**j**	**-i**	-1

Quaternion multiplication is evaluated using the quaternion multiplication rules for the products of two quaternion bases, as shown in Table **1**. Hamilton's quaternion representation of 3D finite rotation is double-valued because it involves the use of half-angles, so that $\mathbf{q}(\theta+2\pi)=-\mathbf{q}(\theta)\neq\mathbf{q}(\theta)$, whereas $\mathbf{q}(\theta+4\pi)=\mathbf{q}(\theta)$.

In Clifford's geometric algebra [15], finite rotations of a 3D vector about an axis in space are effected by an operation involving his non-commutative *geometric multiplication* of an 8-tuple of real numbers $(a_0,a_1,a_2,a_3,a_{23},a_{31},a_{12},a_{123})$ referred to as a *multi-vector*. In 3D a general multi-vector is usually written in the following form, involving the eight multi-vector *bases* $\mathbf{e},\mathbf{e}_1,\mathbf{e}_2,\mathbf{e}_3,\mathbf{e}_{23},\mathbf{e}_{31},\mathbf{e}_{12},\mathbf{e}_{123}$:

$$\mathbf{A} = a_0\mathbf{e} + a_1\mathbf{e}_1 + a_2\mathbf{e}_2 + a_3\mathbf{e}_3 + a_{23}\mathbf{e}_{23} + a_{31}\mathbf{e}_{31} + a_{12}\mathbf{e}_{12} + a_{123}\mathbf{e}_{123} \tag{8}$$

where $a_0\mathbf{e}$ is a scalar, $a_1\mathbf{e}_1+a_2\mathbf{e}_2+a_3\mathbf{e}_3$ is a 3D vector, $a_{23}\mathbf{e}_{23}+a_{31}\mathbf{e}_{31}+a_{12}\mathbf{e}_{12}$ is a 3D bivector, and $a_{123}\mathbf{e}_{123}$ is a 3D trivector. A unit multi-vector (for which $a_0^2+a_1^2+a_2^2+a_3^2+a_{23}^2+a_{31}^2+a_{12}^2+a_{123}^2=1$) is used for the rotation [10]. The geometric multiplication operation that effects the 3D finite rotation of a vector $\mathbf{r}\ (=x\mathbf{e}_1+y\mathbf{e}_2+z\mathbf{e}_3)$ about an axis with direction cosines

(l, m, n) through an angle θ into a new vector $\mathbf{r}'$ $(= x'\mathbf{e}_1 + y'\mathbf{e}_2 + z'\mathbf{e}_3)$, with the same magnitude as the first, is given by:

$$\mathbf{r}' = \mathbf{R}^{\dagger}(\theta)\mathbf{r}\mathbf{R}(\theta) \tag{9}$$

Here the unit multi-vector has the special form, equivalent to that of a *spinor* [16]:

$$\mathbf{R}(\theta) = \cos\frac{\theta}{2}\mathbf{e} + l\sin\frac{\theta}{2}\mathbf{e}_{23} + m\sin\frac{\theta}{2}\mathbf{e}_{31} + n\sin\frac{\theta}{2}\mathbf{e}_{12} \tag{10}$$

consisting of the sum of a scalar and a bivector. Its (multi-vector) *reverse* is,

$$\mathbf{R}^{\dagger}(\theta) = \cos\frac{\theta}{2}\mathbf{e} - l\sin\frac{\theta}{2}\mathbf{e}_{23} - m\sin\frac{\theta}{2}\mathbf{e}_{31} - n\sin\frac{\theta}{2}\mathbf{e}_{12} \tag{11}$$

Table 2. Multiplication Rules for Products of Any Two of the Eight Multi-Vector Bases

$\mathbf{e}$	$\mathbf{e}_1$	$\mathbf{e}_2$	$\mathbf{e}_3$	$\mathbf{e}_{23}$	$\mathbf{e}_{31}$	$\mathbf{e}_{12}$	$\mathbf{e}_{123}$
$\mathbf{e}_1$	$\mathbf{e}$	$\mathbf{e}_{12}$	$-\mathbf{e}_{31}$	$\mathbf{e}_{123}$	$-\mathbf{e}_3$	$\mathbf{e}_2$	$\mathbf{e}_{23}$
$\mathbf{e}_2$	$-\mathbf{e}_{12}$	$\mathbf{e}$	$\mathbf{e}_{23}$	$\mathbf{e}_3$	$\mathbf{e}_{123}$	$-\mathbf{e}_1$	$\mathbf{e}_{31}$
$\mathbf{e}_3$	$\mathbf{e}_{31}$	$-\mathbf{e}_{23}$	$\mathbf{e}$	$-\mathbf{e}_2$	$\mathbf{e}_1$	$\mathbf{e}_{123}$	$\mathbf{e}_{12}$
$\mathbf{e}_{23}$	$\mathbf{e}_{123}$	$-\mathbf{e}_3$	$\mathbf{e}_2$	$-\mathbf{e}$	$-\mathbf{e}_{12}$	$\mathbf{e}_{31}$	$-\mathbf{e}_1$
$\mathbf{e}_{31}$	$\mathbf{e}_3$	$\mathbf{e}_{123}$	$-\mathbf{e}_1$	$\mathbf{e}_{12}$	$-\mathbf{e}$	$-\mathbf{e}_{23}$	$-\mathbf{e}_2$
$\mathbf{e}_{12}$	$-\mathbf{e}_2$	$\mathbf{e}_1$	$\mathbf{e}_{123}$	$-\mathbf{e}_{31}$	$\mathbf{e}_{23}$	$-\mathbf{e}$	$-\mathbf{e}_3$
$\mathbf{e}_{123}$	$\mathbf{e}_{23}$	$\mathbf{e}_{31}$	$\mathbf{e}_{12}$	$-\mathbf{e}_1$	$-\mathbf{e}_2$	$-\mathbf{e}_3$	$-\mathbf{e}$

Geometric multiplication is evaluated using the multi-vector multiplication rules for the products of two multi-vector bases, as shown in Table **2**. Like Hamilton's quaternion method, Clifford's multi-vector representation of 3D finite rotation is double-valued, because it again involves the use of half-angles, so that $\mathbf{R}(\theta + 2\pi) = -\mathbf{R}(\theta) \neq \mathbf{R}(\theta)$, whereas $\mathbf{R}(\theta + 4\pi) = \mathbf{R}(\theta)$.

Hamilton used a combination of a scalar and a vector to form a quaternion representing a 3D rotation. Clifford used a combination of a scalar and a bivector (equivalent to a spinor) to represent a 3D rotation. The quaternion and spinor representations are isomorphic [17].

4. GEOMETRY AND TOPOLOGY OF ROBOT MANIPULATOR PLATFORMS

The geometry of the archetypal Stewart-Gough parallel manipulator [18] is octahedral in the sense that, in a typical position, the moving triangular platform and the fixed triangular base form opposite faces of an octahedron, and the six legs form the edges of the other six triangular faces as shown on the left in Fig. (**4**) [19]. Often the dimensions are such that the moving and fixed platforms are congruent equilateral triangles and in the 'home' position each of the six legs has the same length, equal to the length of the platform edge. In this home position the system forms a regular octahedron, but in most other positions the (polyhedral) regularity is lost and the system has the geometry of a scalene octahedron, although it usually still retains the same topology, defined by its interchange graph.

It is possible to generalise the Stewart-Group platform geometry without changing its topology by re-locating the spherical joints in a 2D polygonal arrangement other than that of an equilateral triangle [20-23]. In general this will form a (non-regular) hexagon. The resulting system then consists of a hexagonal platform moving with respect to a fixed hexagonal base, as shown in the centre in Fig. (**4**). Similar generalisations lead to quadrilateral, pentagonal and, in general, other planar polygonal platforms and bases [2].

A more radical generalisation to form a 3D spatial (i.e. non-planar) arrangement of the spherical joints is possible, where the joints on the moving 'platform' are located at the vertices of a (not necessarily regular) octahedron, as illustrated on the right in Fig. (**4**) [3]. The joints on the fixed 'base' are similarly arranged at the vertices of a different octahedron that encloses the first and this is illustrated in transparent outline again on the right in Fig. (**4**). The resulting system then has a more general geometry than previous types of parallel robot manipulator derived from the Stewart-Gough platform. In this case the actual moving 'platform', without the legs, is itself a rigid octahedron (rather than an equilateral triangle or hexagon, as previously). This very general type of parallel manipulator system is referred to as a 6-legged 3D octahedral platform.

Further generalisations of platform geometry (keeping the same topology) are possible by introducing different numbers, types and sequences of joints along each leg to produce redundant systems in general. Furthermore, the topology of parallel manipulators may be changed by altering the number of legs, and of course the special case with just one leg clearly reduces to a serial manipulator. Of course some of the links may be struts, ties or cables so that these generalisations are just as valid for tensegrity-based and cable-based parallel manipulator systems.

The functioning of each of these types of manipulator system must be constrained by the fundamental nature of 3D motion. Surprisingly, this includes the double-valued aspect of finite rotations, as revealed by the parametric ball representation and the quaternion and spinor representations discussed in Sections 2 and 3. Ostensibly it does not seem possible that mechanical manipulators may exhibit this aspect, regardless of their geometry and topology. This is particularly puzzling in the case of multi-legged systems, where intuitively it appears that the legs (whether consisting of rigid links or cables) would become hopelessly entangled after a 4π rotation and would 'obviously' be in a different configuration than they would be after a zero rotation. This apparent impossibility is dismissed and resolved by examining the rotation of 2-legged, 3-legged, and 6-legged systems.

5. THE DIRAC MODEL FOR 2-, 3-, AND 6-LEGGED PLATFORMS

In an attempt to find a classical-mechanical analogue for the quantum mechanical property of electron spin Dirac [11] constructed a mechanical model that physically demonstrated the inequivalence of zero and 2π rotations in 3D. The

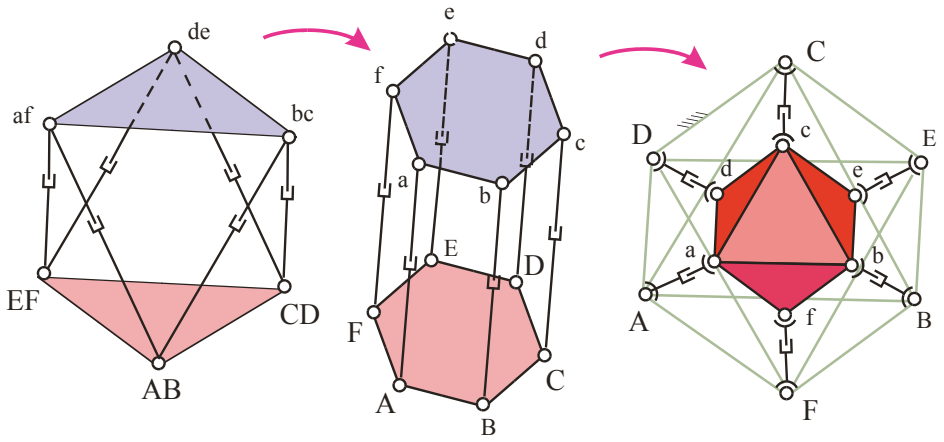

Fig. (4). Three types of 6-6 parallel manipulator geometry, progressively more generalised.

device consisted of a relatively large cubic framework within which a smaller cube was located. The smaller cube was connected to the larger cube by eight elastic strings, such that each string joined a vertex of the inner cube to the corresponding vertex of the outer cube. The arrangement was very similar to that for the two nested octahedra shown on the right of Fig. (**4**). If Dirac's inner cube is rotated with respect to the outer cube through an angle of 2π about a vertical axis the eight elastic strings become entangled. With the inner cube held in this position any attempt to untangle the strings fails. Of course, reversing the rotation does return the configuration to its initial untangled state. The surprising feature of the device is that a rotation of the inner cube through an angle of 4π from its initial pose leads to a configuration that can be untangled, despite the fact that it appears to produce an even more entangled state.

The similarity of the Dirac model to the octahedral manipulator platform of Fig. (**4**) is suggestive and indeed their behaviour is analogous. If the six legs of the octahedral manipulator are replaced with elastic cables (or highly redundant serial kinematic chains) then Dirac's procedure may be applied directly to the system. If the inner octahedron is rotated through 2π it is found that just as with Dirac's model, the legs cannot be untangled, and the system is in a different state from its initial (un-rotated) state. However, if the inner octahedron is rotated through 4π and then held in position to prevent reversal of the rotation, it is possible to untangle the legs and return directly to the initial state. Hence the initial zero-rotation state is equivalent to the 4π-rotation state but not to the 2π-rotation state.

The process of untangling the legs is essentially independent of the number of legs and it is also not dependent on their geometrical juxtaposition. The procedure may be outlined more easily by considering the slightly simpler case of a circular disc platform attached to a circular disc fixed base by various numbers of legs (elastic cables). For the 2-legged system shown in Fig. (**5**) the situation is straightforward. As viewed from above, the platform is rotated with respect to the fixed base anti-clockwise about a vertical axis through an angle of 2π and held in this pose. The effect on the cables is to twist them into a right-handed helical configuration. If the cables are now grasped together and passed over the top of the platform, they do not untangle but instead become twisted into a left-handed helical configuration. However, if the platform is returned to its initial state and then rotated with respect to the base anti-clockwise about a vertical axis through an angle of 4π, the cables *are* untangled by the above procedure.

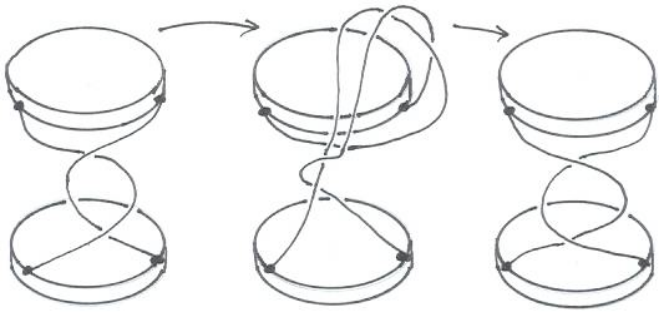

Fig. (5). An attempt at untangling the legs of a 2-legged platform after a 2π rotation.

In the case of the 3-legged system shown in Fig. (**6**) the process is essentially the same as for the previous 2-legged system in Fig. (**5**). A 2π rotation produces a tangled configuration of the three cables whereas a 4π rotation produces a tangled configuration that may be untangled (without rotating the platform) by passing the three cables over the top of the platform, either one at a time, or all three together. Note that for clarity and ease of drawing the central image in Fig. (**6**) is shown with the three (tangled) cables partly shrouded in a 'sleeve'.

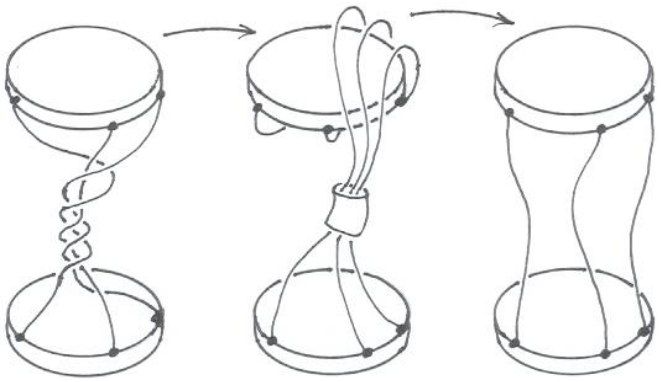

Fig. (6). Untangling the legs of a 3-legged platform after a 4π rotation.

In a similar way a platform supported by six legs from a base, or indeed an m-legged system of this type (m>6), may have all of its legs untangled after a 4π rotation by passing all of the cables over the top of the platform. The process shown in Fig. (**6**) continues to be applicable for six (or for an arbitrary number of) legs.

However, the type of 6-legged system just described differs from the octahedral platform shown on the right in Fig. (**4**) in having the base and all six legs 'below' the platform. Now consider the slightly modified circular disc platform configuration shown in Fig. (**7**), where the fixed base consists of two separated circular discs, one fixed above and one fixed below the platform, with three legs attached from the platform to each of these two base discs.

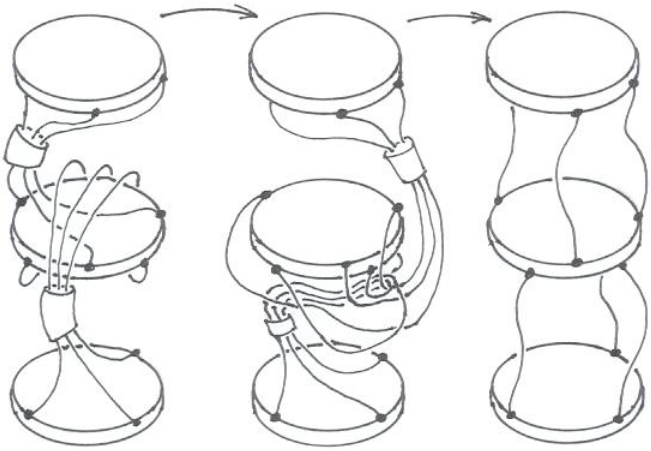

Fig. (7). Untangling the legs of a 6-legged platform after a 4π rotation.

This is much closer to the octahedral arrangement shown on the right of Fig. (**4**). As before the platform may be rotated, with respect to the fixed bases, anti-clockwise about a vertical axis through an angle of 4π. This results in the three lower cables being twisted into a right-handed helical configuration, whereas the three upper cables are twisted into a left-handed helical configuration. Now the untangling procedure should be applied in two stages, but it is just as successful at untangling the cables. Firstly, the three lower cables (again shown wrapped in a sleeve for clarity) are passed over the top of the platform. This completes the first stage and it now appears that the three lower cables are hopelessly entangled with the three upper cables. The second stage of the process entails passing the three upper cables underneath the platform, and surprisingly this completely untangles all six cables. Needless to say, after just a 2π rotation of the platform with respect to the base(s) the procedure will not untangle the cables, nor will any similar procedure that does not cut the cables nor rotate the platform.

6. DISCUSSION AND CONCLUSIONS

The procedures introduced in this paper have implications for the kinematic design and operation of parallel and hybrid parallel-serial robot manipulator systems. They demonstrate, for instance, that the state of a platform depends fundamentally not only on its spatial finite *displacement* from one pose to another pose and configuration, but also on the *history* of its spatial *motion*. A platform in any one pose may have achieved that pose in two inequivalent ways – by rotation through $4n\pi$, or by rotation through $(4n+2)\pi$, where n is any integer (positive, negative or zero). Hence, every pose of a platform is in one of two states, depending on the previous motion history of the platform. The two states are manifested by the two theoretically possible configurations of the legs ('tangled' and 'untangled') connecting the platform to the base. However, for this feature to be realised in an actual mechanical system, the legs would have to be so designed that they allowed the platform to rotate through at least 4π with respect to the base. This would probably require the legs to have unusual shapes and to have (many) redundant freedoms so that they almost behaved as cables. Currently the designs of most manipulators prevent such unrestrained rotations.

For serial manipulators (1-legged platform systems) these aspects are not generally manifested overtly (but would be if power- and instrumentation- cabling or hydraulic lines were taken into account). For m-legged parallel manipulators (m>1) an untangling procedure might be exploited to produce, for instance, continuous rotation of the platform about a vertical axis through as many full turns as desired without entangling the legs, assuming the legs are 'flexible enough' to go through the untangling procedure for every 4π of rotation angle. This possibility may be seen most clearly in the case of a 2-legged system. If the two legs were viewed either as two separate cables or else as the two edges of a ribbon cable (for example), there could be continuous rotation of the platform with respect to the base without the cable(s) becoming irretrievably coiled. This would provide a way for a rotor to rotate continuously with respect to a stator without the need for slip-rings or commutators.

Such a system has actually been designed and successfully patented by Adams [24, 25] in the context of providing (electrical) energy communication between a moving and a stationary terminal. His purpose was to avoid the use of commutators and slip-rings because these generate increasingly unacceptable levels of electrical noise as electronic systems are miniaturised. The construction utilises a gear train involving a 2:1 gear ratio and it provides a novel mechanical arrangement for continuously untangling the cables. It is effective but there is considerable scope for improvement in its mechanical features. Adams' patent [25] also shows application to pneumatic and hydraulic connections and to folded optical systems involving sequences of prisms. Moreover, it could provide a practical means of rotating the revolute joints of a serial manipulator through any number of complete turns without their angular range being restricted by power-cable or sensor-cable constraints. Its utilisation in the design of parallel manipulators is a natural extension.

Further work is planned to explore the implications of this approach for the detailed geometry, topology and mechanical configurations of new types of robot manipulator designs. In particular, the mobility, dexterity and redundancy aspects required of platform legs, in order for them to be able to execute an untangling procedure, are expected to form a major focus for future exploration. Additionally, the implications for more general *screw* motion (rather than just for rotational motion) will be explored in several follow-up papers.

REFERENCES

[1] M. Hiller, S. Fang, S. Mielczarek, R. Verhoeven, and D. Franitza, "Design, analysis and realization of tendon-based parallel manipulators", *Mechanism and Machine Theory*, vol. 40, pp. 429-445, 2005.

[2] J. Rooney, J. Duffy, and J. Lee, "Tensegrity and compegrity configurations in anti-prism manipulator platforms", in *Proceedings of the Tenth World Congress on the Theory of Machines and Mechanisms*, Oulu, Finland, 1999, pp. 1278-1287.

[3] T. K. Tanev, and J. Rooney, "Rotation symmetry axes and the quality index in a 3D octahedral Parallel Robot Manipulator System". In *Advances in Robot Kinematics: Analysis and Control*, J. Lenarcic, and F. Thomas, Eds. Dordrecht: Kluwer Academic Publishers, 2002, pp. 29-38.

[4] J. Rooney, "A survey of representations of spatial rotation about a fixed point", *Environment and Planning B*, vol. 4, pp. 185-210, 1977.

[5] J.B. Kuipers, *Quaternions and Rotation Sequences: A Primer with Applications to Orbits, Aerospace and Virtual Reality,* Princeton: Princeton University Press, 1999.

[6] D.F. Rogers, and J.A. Adams, *Mathematical Elements for Computer Graphics,* New York: McGraw-Hill, 1976.

[7] J. Rooney, "On obtaining the velocity motor of any link in a general *n*-link spatial manipulator", in *Proceedings of the Fourth World Congress on the Theory of Machines and Mechanisms*, Newcastle-upon-Tyne, England, 1975, pp. 1083-1087.

[8] P.A.M. Dirac, *The Principles of Quantum Mechanics*, Oxford: Clarendon Press, 1958.

[9] H. Weyl, *The Theory of Groups and Quantum Mechanics*, London: Methuen, 1931.

[10] D. Hestenes, *New Foundations for Classical Mechanics,* Dordrecht: Kluwer Academic Publishers, 1986.

[11] C.W. Misner, K. S. Thorne, and J. A. Wheeler, *Gravitation*, San Francisco: W H Freeman, 1970.

[12] I.R. Porteous, *Topological Geometry*, Cambridge: Cambridge University Press, 1969.

[13] S.L. Altmann, *Rotations, Quaternions, and Double Groups,* Oxford: Clarendon Press, 1986.

[14] W.R. Hamilton, *Elements of Quaternions,* Cambridge: Cambridge University Press, 1899.

[15] W.K. Clifford, *Mathematical Papers*, R. Tucker, Ed. New York: Chelsea Publishing Company, 1968 [reprint of 1882 first edition].

[16] E. Cartan, *The Theory of Spinors*. New York: Dover Publications, 1981 [reprint of 1966 English translation, Hermann, Paris, of original 1937 French edition].

[17] J. Rooney, "Multivectors and quaternions in rigid body rotation: Clifford vs. Hamilton", in *Proceedings of the Twelfth World Congress in Mechanism and Machine Science*, Besancon, France, 2007.

[18] D. Stewart, "A platform with six degrees of freedom", in *Proceedings of Institution of Mechanical Engineers*, London, UK, vol. 180, no. 15, pp. 371-386, 1965.

[19] J. Lee, J. Duffy, and K. H. Hunt, "A practical quality index on the octahedral manipulator", *International Journal of Robotics Research*, vol. 17, no. 10, pp. 1081-1090, 1998.

[20] J. Duffy, J. Rooney, B. Knight, and C. D. Crane, "A review of a family of self-deploying tensegrity structures with elastic ties", *Shock and Vibration Digest*, vol. 32, no. 2, pp. 100-106, 2000.

[21] J-P. Merlet, "Direct kinematics of parallel manipulators", *IEEE Transactions on Robotics and Automation*, vol. 9, no. 6, pp. 842-846, 1993.

[22] B. Mayer St-Onge, and C. M. Gosselin, "Singularity analysis and representation of the general Gough-Stewart platform", *International Journal of Robotics Research*, vol. 19, no. 3, pp. 271-288, 2000.

[23] K.E. Zanganeh, and J. Angeles, "Kinematic isotropy and optimum design of parallel manipulators", *International Journal of Robotics Research*, vol. 16, no. 2, pp. 185-197, 1997.

[24] C.L. Strong, "The Amateur Scientist: … how to supply electric power to something that is turning", *Scientific American*, vol. 233, no. 6, pp. 120-125, December 1975.

[25] D.A. Adams, "*Apparatus for providing energy communication between a moving and a stationary terminal*", United States Patent # 3586413, June 21, 1971.

Received: May 08, 2010 Revised: June 18, 2010 Accepted: June 29, 2010